Task space controller for the novel Active Ankle

Shivesh Kumar, Bertold Bongardt, Marc Simnofske, Frank Kirchner
Robotics Innovation Center (RIC), DFKI, Bremen, Germany

Introduction

ACTIVE ANKLE is a novel parallel manipulator with three degrees of freedom that operates in an almost-spherical manner [1, 2]. The almost-spherical parallel manipulator (ASPM) is primarily intended as an actuated ankle joint in a full-body exoskeleton for rehabilitation application (Fig. 3).

Design features

1. lightweight and robust construction
2. modular design leading to low link diversity
3. high stiffness and orientation accuracy
4. high payload capacity
5. no torques required for loads along torsional axis

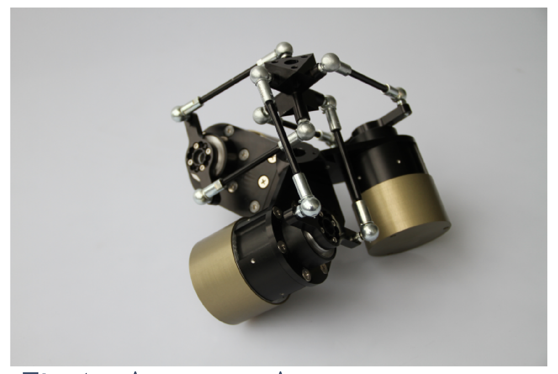

Fig.1: ACTIVE ANKLE prototype

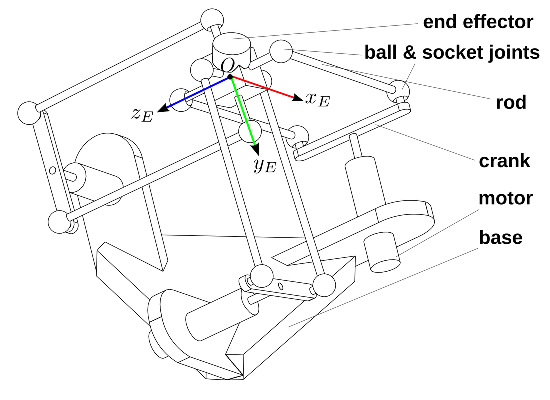

Fig.2: Sketch of the ACTIVE ANKLE

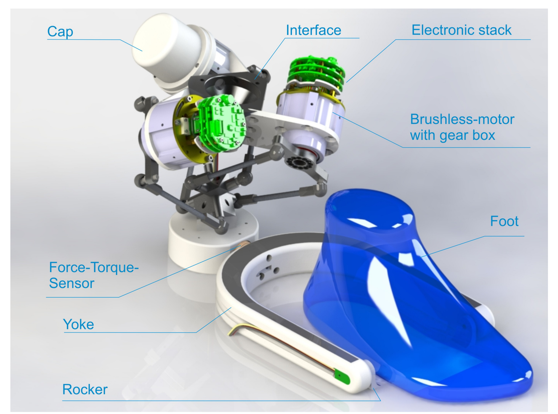

Fig.3: ACTIVE ANKLE with foot unit

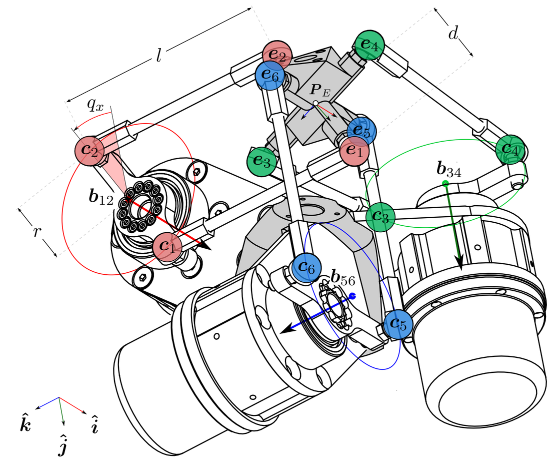

Fig.4: Scheme, $r = d = 35$, $l = 100$.

Control challenge

Due to spatial behaviour but spherical use case of the ACTIVE ANKLE, the task space control of this mechanism asks for a joint configuration for a given orientation from $SO(3)$, instead of a pose from $SE(3)$ [3].

Inverse Geometric Model (IGM)

The Inverse Geometric Model (IGM) is a solution to the problem of finding input joint angles $[q_x, q_y, q_z]$ for a specific end-effector pose $\mathbf{P}_E = \begin{bmatrix} \mathbf{s} & \mathbf{n} & \mathbf{a} & \mathbf{e} \\ 0 & 0 & 0 & 1 \end{bmatrix} \in SE(3)$, denoted as

$$[q_x, q_y, q_z] = \mathrm{IGM}(\mathbf{P}_E), \quad \mathbf{P}_E \in SE(3) .$$

Crank & endeffector points

The crank points $(\mathbf{c}_1, \mathbf{c}_2, \mathbf{c}_3, \mathbf{c}_4, \mathbf{c}_5, \mathbf{c}_6)$ are allowed to move on the circles defined by the motion of three actuators. The end effector points $(\mathbf{e}_1, \mathbf{e}_2, \mathbf{e}_3, \mathbf{e}_4, \mathbf{e}_5, \mathbf{e}_6)$ lie on a sphere of radius d and center $\mathbf{e}$.

The point parametrizations (CPL & EPL) are:

$$\mathbf{c}_1 = [0, r\cos(q_x), l + r\sin(q_x)]^T \qquad \mathbf{e}_1 = \mathbf{e} + d \cdot \mathbf{n}$$
$$\mathbf{c}_2 = [0, r\cos(q_x), l - r\sin(q_x)]^T \qquad \mathbf{e}_2 = \mathbf{e} - d \cdot \mathbf{n}$$
$$\mathbf{c}_3 = [l + r\sin(q_y), 0, r\cos(q_y)]^T \qquad \mathbf{e}_3 = \mathbf{e} + d \cdot \mathbf{s}$$
$$\mathbf{c}_4 = [l - r\sin(q_y), 0, r\cos(q_y)]^T \qquad \mathbf{e}_4 = \mathbf{e} - d \cdot \mathbf{s}$$
$$\mathbf{c}_5 = [r\cos(q_z), l + r\sin(q_z), 0]^T \qquad \mathbf{e}_5 = \mathbf{e} + d \cdot \mathbf{a}$$
$$\mathbf{c}_6 = [r\cos(q_z), l - r\sin(q_z), 0]^T \qquad \mathbf{e}_6 = \mathbf{e} - d \cdot \mathbf{a} .$$

Constraint equations

Expansion of contraint equations $\|\mathbf{e}_i - \mathbf{c}_i\| = l$ yields

$$(e_x + d\cdot n_x)^2 + (e_y + d\cdot n_y - r\cdot\cos q_x)^2 + (e_z + d\cdot n_z - l - r\cdot\sin q_x)^2 = l^2 \quad (1)$$
$$(e_x - d\cdot n_x)^2 + (e_y - d\cdot n_y + r\cdot\cos q_x)^2 + (e_z - d\cdot n_z - l + r\cdot\sin q_x)^2 = l^2 \quad (2)$$
$$(e_x + d\cdot a_x - l - r\cdot\sin q_y)^2 + (e_y + d\cdot a_y)^2 + (e_z + d\cdot a_z - r\cdot\cos q_y)^2 = l^2 \quad (3)$$
$$(e_x - d\cdot a_x - l + r\cdot\sin q_y)^2 + (e_y - d\cdot a_y)^2 + (e_z - d\cdot a_z + r\cdot\cos q_y)^2 = l^2 \quad (4)$$
$$(e_x + d\cdot s_x - r\cdot\cos q_z)^2 + (e_y + d\cdot s_y - l - r\cdot\sin q_z)^2 + (e_z + d\cdot s_z)^2 = l^2 \quad (5)$$
$$(e_x - d\cdot s_x + r\cdot\cos q_z)^2 + (e_y - d\cdot s_y - l + r\cdot\sin q_z)^2 + (e_z - d\cdot s_z)^2 = l^2 \quad (6)$$

Three virtual leg equations

By subtracting (2) from (1), (4) from (3), (6) from (5), three virtual leg equations are derived

$$re_y\cos(q_x) + r(e_z - l)\sin(q_x) + d(ln_z - \mathbf{e}*\mathbf{n}) = 0$$
$$re_z\cos(q_y) + r(e_x - l)\sin(q_y) + d(la_x - \mathbf{e}*\mathbf{a}) = 0$$
$$re_x\cos(q_z) + r(e_y - l)\sin(q_z) + d(ls_y - \mathbf{e}*\mathbf{s}) = 0 .$$

With leg index $j \in \{1, 2, 3\}$, they are of the form

$$E_j \cdot \cos(q_j) + F_j \cdot \sin(q_j) + G_j = 0 . \quad (7)$$

IGM Solution

By tangent half angle substitution $t_j = \tan(q_j/2)$, $\cos q_j = (1 - t_j^2)/(1 + t_j^2)$, $\sin q_j = 2t_j/(1 + t_j^2)$, the equation

$$(G_j - E_j)\cdot t_j^2 + 2\cdot F_j \cdot t_j + (G_j + E_j) = 0$$

in t is obtained. The two solutions for q_j are given by

$$q_{j_+}, q_{j_-} = 2\cdot \mathrm{atan2}(-F_j \pm H_j, G_j - E_j)$$

with $H_j = \sqrt{E_j^2 + F_j^2 - G_j^2}$, see [3].

Rotative Inverse Geometric Model (RIGM)

Rotative Inverse Geometric Model (RIGM) is to find input joint angles for a desired orientation of the endeffector $\mathbf{R}_E$ without knowledge of the end-effector position as

$$[q_x, q_y, q_z] = \mathrm{RIGM}(\mathbf{R}_E), \quad \mathbf{R}_E \in SO(3) .$$

RIGM solution

Equations (1) - (6) are highly coupled. A novel iterative algorithm has been developed which can be explained by the concept of virtual joints. The method TFGM implements a three-sphere intersection to solve for $\mathbf{e}$ [3].

Algorithm 1 Rotative Inverse Geometric Model (RIGM)

(in) Desired orientation of the end effector, $\mathbf{R}_E$
(out) Input joint angles $[q_x, q_y, q_z]$ and EE shift $[e_x, e_y, e_z]$

```
1:  function RIGM(R_E, ε)
2:      P̃_E ← [R_E 0_3×1; 0_1×3 1]                ▷ Initialization
3:      while E_LS < ε do
4:          (ẽ_1 ... ẽ_6) ← EPL(P̃_E)
5:          [q̃_x, q̃_y, q̃_z] ← IGM(P̃_E)
6:          (c̃_1 ... c̃_6) ← CPL(q̃_x, q̃_y, q̃_z)
7:          E_LS ← Σ_i^6 (||ẽ_i − c̃_i|| − l)^2        ▷ Error
8:          ẽ ← TFGM(q̃_x, q̃_y, q̃_z, R_E)
9:          P̃_E ← [R_E ẽ_3×1; 0_1×3 1]               ▷ Update
10:     [q_x, q_y, q_z] ← [q̃_x, q̃_y, q̃_z]
11:     [e_x, e_y, e_z] ← [ẽ_x, ẽ_y, ẽ_z]
12:     return [q_x, q_y, q_z, e_x, e_y, e_z]
```

Range of motion (ROM) comparison

During most activities of daily living, only partial ranges of motion required [4], e.g, $10^\circ - 15^\circ$ plantar flexion and 10° dorsiflexion for walking on even surfaces, walking upstairs (37° total ROM), walking downstairs (56° total ROM).

Fig.1: Comparison of ROM between human and ACTIVE ANKLE.

Motion type	Human Ankle			ACTIVE ANKLE		
	min.	max.	abs.	min.	max.	abs.
DF – PF	−20°	50°	70°	−19.83°	37.23°	57.06°
EV – IV	−15°	35°	50°	−14.62°	34.84°	49.46°
AD – AB	−30°	45°	75°	−29.20°	36.96°	66.16°

Experimental results

RIGM has been implemented for a task space control of the ACTIVE ANKLE. For $\epsilon = 1.e^{-06}$ mm, the algorithm can be realized at a control frequency of 10 kHz [3].

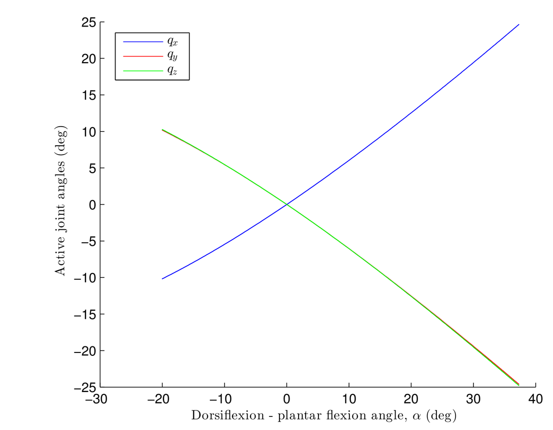

Fig.5: Active joint angles during the dorsiflexion – plantarflexion motion.

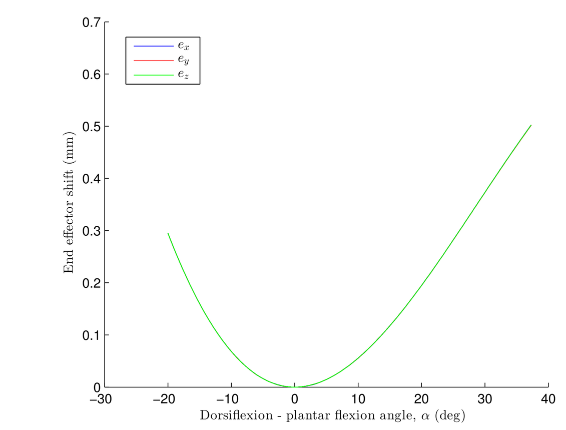

Fig.6: End effector shift during the dorsiflexion – plantarflexion motion.

Inverse Kinematics

The three virtual leg equations (7) can be differentiated with respect to time and can be rearranged as a relation between twist ($\mathbf{t}$) and actuated joint velocities ($\dot{\mathbf{q}}$) through serial ($\mathbf{B}$) and parallel ($\mathbf{A}$) Jacobian matrices:

$$\mathbf{A}\cdot\mathbf{t} = \mathbf{B}\cdot\dot{\mathbf{q}}$$

The solution of the Inverse Kinematics problem requires:

$$\dot{\mathbf{q}} = \mathbf{B}^{-1}\cdot\mathbf{A}\cdot\mathbf{t}$$

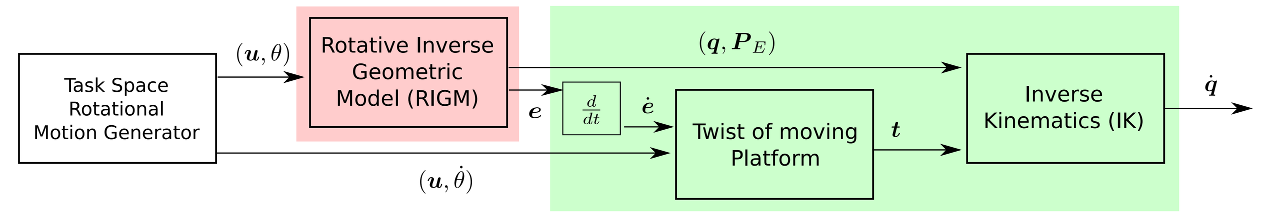

Fig.7: Cascaded task-space position and velocity control using RIGM and IK

Task-space cascaded control

The joint-based FPGA stacks implement cascaded position, velocity and torque control. An equivalent control framework is envisioned in 3-DoF spherical task space which makes it a compact and versatile rehabilitation device.

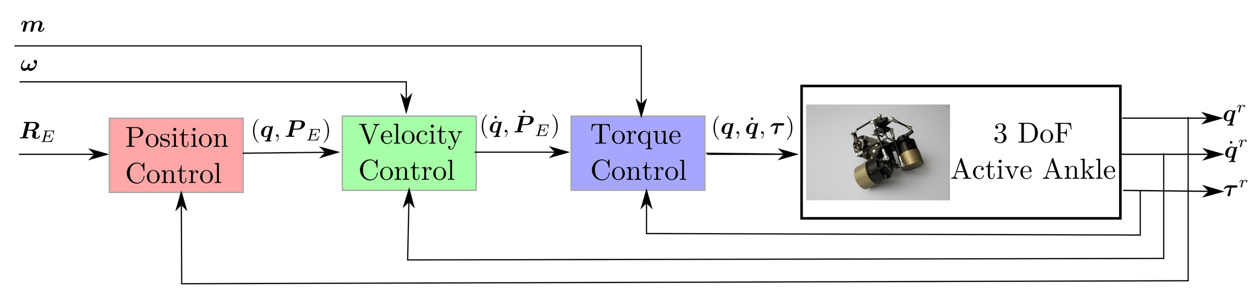

Fig.8: Cascaded task-space control scheme: a combination of desired orientation ($\mathbf{R}_E$), angular velocity (ω) and moments ($\mathbf{m}$) in $SO(3)$ can be the inputs.

Conclusions

The novel ACTIVE ANKLE mechanism is briefly presented along with relevant geometric and kinematic models for its control in task-space. In the future, the cascaded task-space control framework will be equipped with torque control.

Acknowledgment

The work presented in this paper was performed within the project Recupera-Reha, funded by the German Aerospace Center (DLR) with federal funds from the Federal Ministry of Education and Research (BMBF) (Grant 01-IM-14006A).

RECUPERA REHA

Federal Ministry of Education and Research

References

[1] M. Simnofske. *Ausrichtungsvorrichtung zum Ausrichten einer Plattform in drei rotatorischen Freiheiten*. Patent application, DE102013018034A1. 2015.

[2] Marc Simnofske et al. "Active Ankle - an Almost-Spherical Parallel Mechanism". In: *Proceedings of ISR 2016: 47st International Symposium on Robotics*. 2016, pp. 1–6.

[3] Shivesh Kumar et al. "Geometric Analysis and Characterization of the Almost Spherical Active Ankle". In: *Mechanism and Machine Theory* (2016). Under Review.

[4] Richard N. Stauffer, Edward Y. S. Chao, and Robert C. Brewster. "Force and Motion Analysis of the Normal, Diseased, and Prosthetic Ankle Joint". In: *Clinical Orthopaedics and Related Research* 127.127 (1977), pp. 189–96.